

SUPPORTING INFORMATION

Supporting Information

SnS@C nanospheres coated with few-layer MoS₂ nanosheets and nitrogen, phosphorus-codoped carbon as robust sodium ion battery anodes

Yuyu Wang,^{a‡} Wenpei Kang,^{b‡*} Ping Ma,^a Dongxu Cao,^a Dongwei Cao,^a Zixi Kang,^b Daofeng Sun^{ab*}

^a College of Science, China University of Petroleum (East China), Qingdao, Shandong 266580, People's Republic of China.

^b School of Materials Science and Engineering, China University of Petroleum (East China), Qingdao, Shandong 266580, People's Republic of China.

*Email: wpkang@upc.edu.cn; dfsun@upc.edu.cn

The supporting information contains Fig. S1-S9 and Table S1-S3.

‡ These authors contributed equally to this work.

SUPPORTING INFORMATION

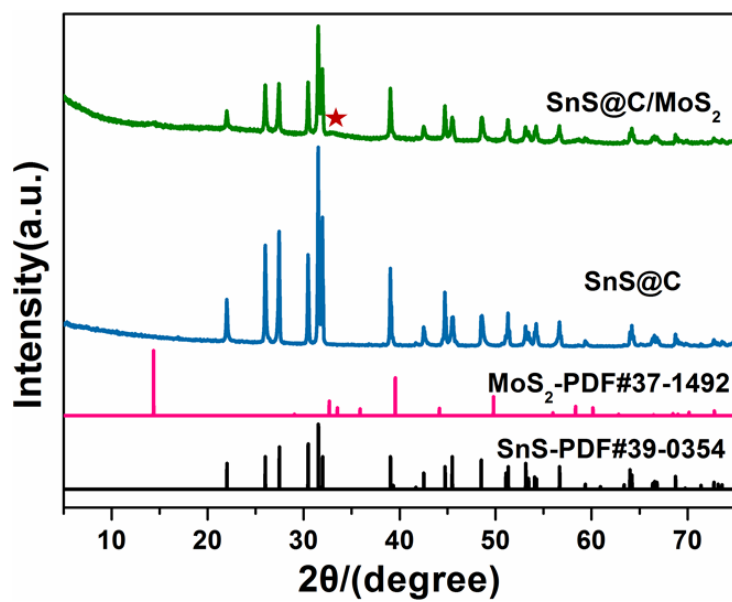


Fig. S1 XRD patterns of SnS@C and SnS@C/MoS₂.

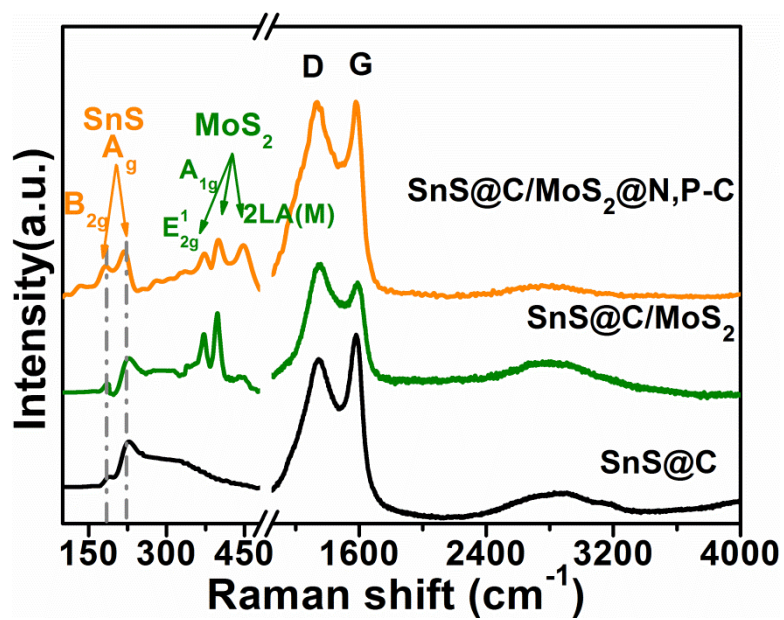


Fig. S2 Comparison of the Raman spectra for SnS@C, SnS@C/MoS₂ and SnS@C/MoS₂@N,P-C.

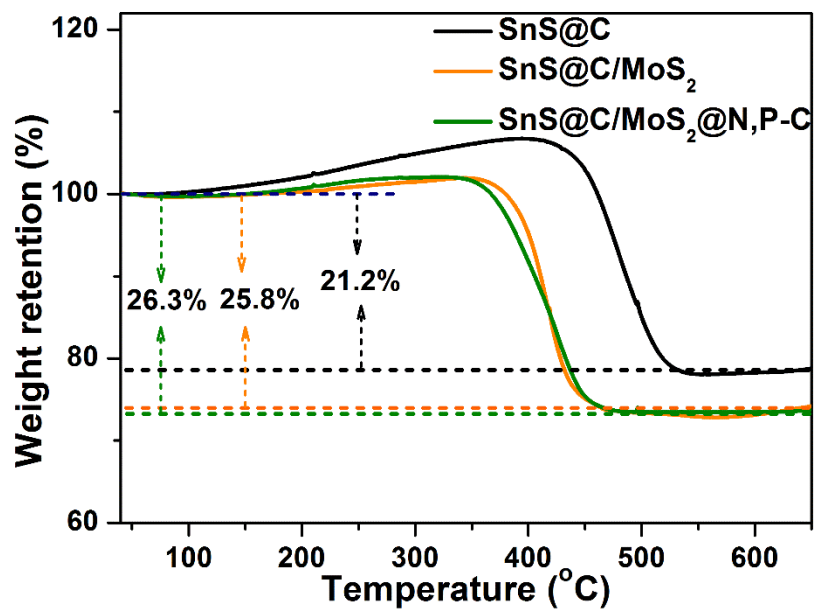


Fig. S3 Comparison of the TGA curves for SnS@C, SnS@C/MoS₂ and SnS@C/MoS₂@N,P-C.

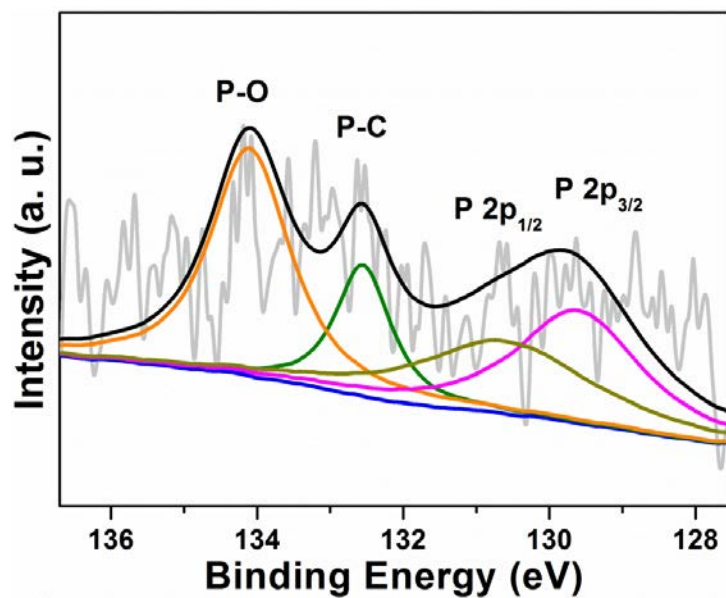


Fig. S4 High-resolution XPS spectra of P 2p in SnS@C/MoS₂@N,P-C composite.

SUPPORTING INFORMATION

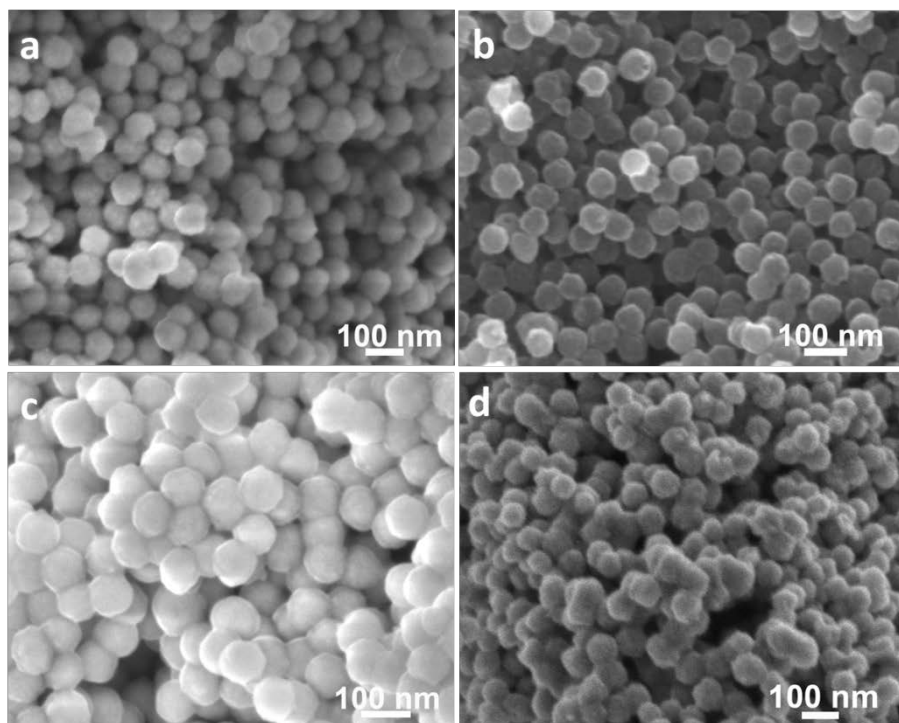


Fig. S5 SEM images of (a) $\text{SnO}_2@\text{C}$ precursor, (b) $\text{SnS}@ \text{C}$, (c) $\text{SnO}_2@\text{C}/\text{PPy-PMo}_{12}$, (d) $\text{SnS}@ \text{C}/\text{MoS}_2$.

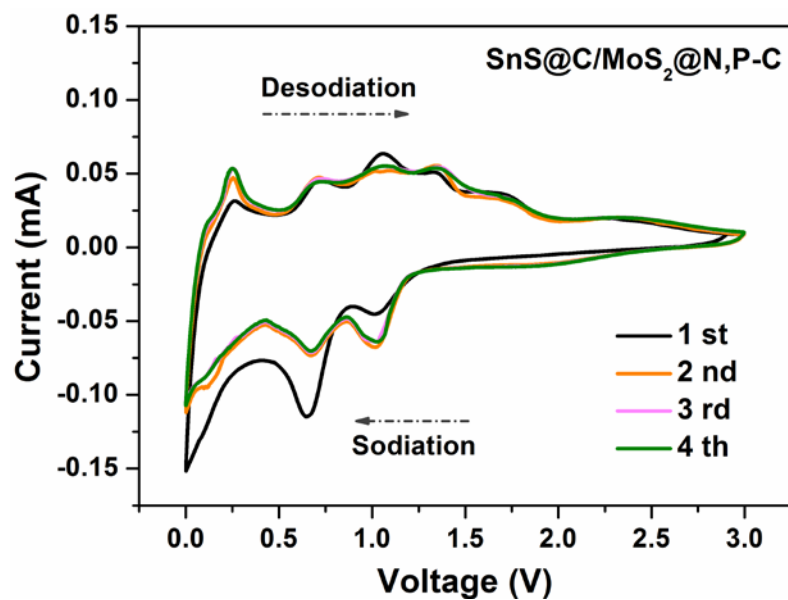


Fig. S6 CV curves at a scan rate of 0.1 mV s^{-1} for SnS@C/MoS₂@N,P-C composite.

SUPPORTING INFORMATION

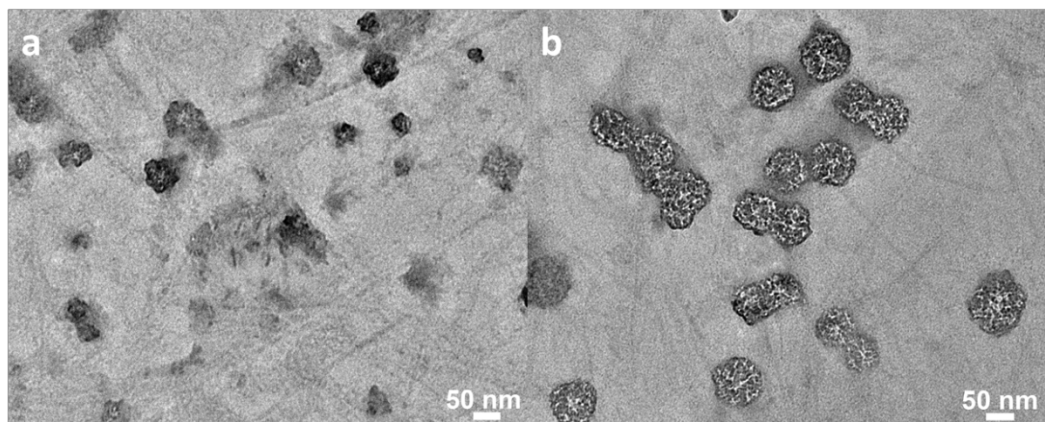


Fig. S7 TEM images of (a) SnS@C electrode, (b) SnS@C/MoS₂@N,P-C composite electrode after charge-discharge cycling.

SUPPORTING INFORMATION

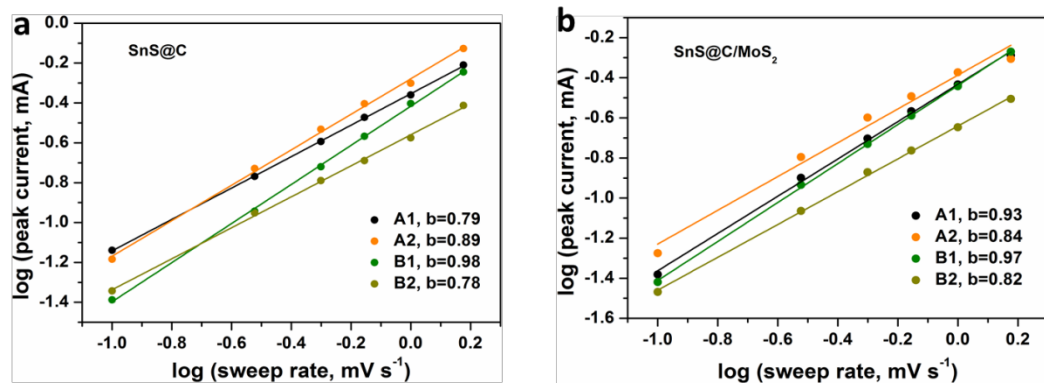


Fig. S8 b-value analyses of (a)SnS@C and (b) SnS@C/MoS₂ based on the relationship between the peak currents and the scan rates.

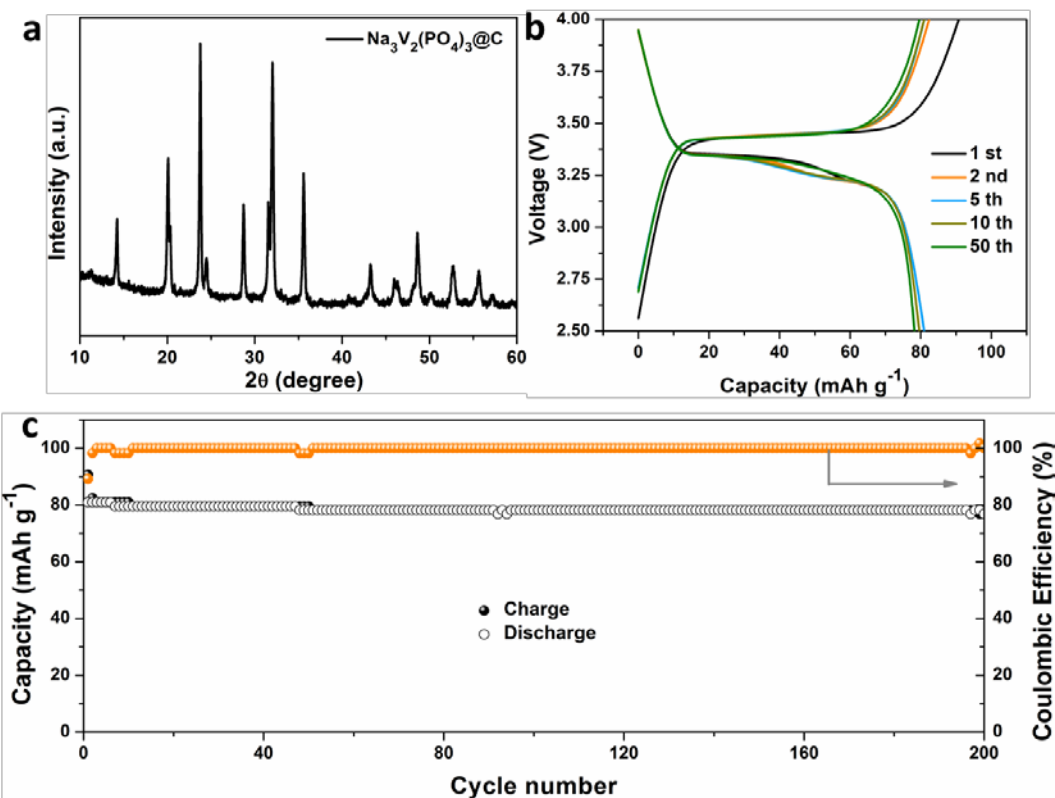


Fig. S9 (a) XRD pattern of the homemade NVP@C. (b) Galvanostatic charge and discharge curves. (c) Cycling performance of NVP@C half cells at 500 mA g^{-1} .

SUPPORTING INFORMATION

Table S1. ICP result of the SnS@C/MoS₂@N,P-C nanocomposite.

Analyte	Conc.Units
Sn	3.026 mg/L
Mo	1.754 mg/L

SUPPORTING INFORMATION

Table S2. Electrochemical performance of the reported SnS-based nanostructures as anode materials for SIBs.

Materials	Rate capacity (mA h g ⁻¹)	Initial Coulombic efficiency (%)	References
SnS@C/MoS ₂ @N,P-C	577 mA h g ⁻¹ at 0.1 A g ⁻¹ 250 mA h g ⁻¹ at 10.0 A g ⁻¹	74.9%	This work
SnS@C/MoS ₂	519 mA h g ⁻¹ at 0.1 A g ⁻¹ 217 mA h g ⁻¹ at 10.0 A g ⁻¹	72.1%	This work
SnS@C	539 mA h g ⁻¹ at 0.1 A g ⁻¹ 192 mA h g ⁻¹ at 10.0 A g ⁻¹	67.8%	This work
SnS@C-rGO	825 mA h g ⁻¹ at 0.1 A g ⁻¹ 336 mA h g ⁻¹ at 1.6 A g ⁻¹	62.0%	[S1]
SnS HNFs	615 mA h g ⁻¹ at 0.1 A g ⁻¹ 228 mA h g ⁻¹ at 2.0 A g ⁻¹	48.3%	[S2]
SnS@SPC	512 mA h g ⁻¹ at 0.1 A g ⁻¹ 235 mA h g ⁻¹ at 3.2 A g ⁻¹	64.6%	[S3]
C@SnS-rGO	534.6 mA h g ⁻¹ at 0.1 A g ⁻¹ 287.6 mA h g ⁻¹ at 3.2 A g ⁻¹	66.0%	[S4]
SnS/SnSb@C	458 mA h g ⁻¹ at 0.1 A g ⁻¹ 159 mA h g ⁻¹ at 2.0 A g ⁻¹	62.5%	[S5]
3D SnS/N-CNNs	791 mA h g ⁻¹ at 0.1 A g ⁻¹ 265 mA h g ⁻¹ at 5.0 A g ⁻¹	70.4%	[S6]
C@SnS/SnO ₂ @Gr	520 mA h g ⁻¹ at 0.81 A g ⁻¹ 430 mA h g ⁻¹ at 2.43 A g ⁻¹	74.6%	[S7]
SnS@RGO	457 mA h g ⁻¹ at 0.02 A g ⁻¹ 240 mA h g ⁻¹ at 0.4 A g ⁻¹	60.0%	[S8]
NBT/C@MoS ₂ NFs	474.5 mA h g ⁻¹ at 0.1 A g ⁻¹ 258.3 mA h g ⁻¹ at 2.0 A g ⁻¹	50.3%	[9]
Ex-MoS ₂ /RGO@C	466 mA h g ⁻¹ at 0.1 A g ⁻¹ 316 mA h g ⁻¹ at 2.0 A g ⁻¹	66.3%	[10]
Fe _{1-x} S/MoS ₂	637.2 mA h g ⁻¹ at 0.1 A g ⁻¹ 372.1 mA h g ⁻¹ at 3.0 A g ⁻¹	60.0%	[11]
Co-doped 1T-MoS ₂ /NSC	459.4 mA h g ⁻¹ at 0.2 A g ⁻¹ 235.9 mA h g ⁻¹ at 25 A g ⁻¹	67.5%	[12]

SUPPORTING INFORMATION

$\text{MoS}_2\text{-C@C}$	583 mA h g^{-1} at 0.1 A g^{-1} 164 mA h g^{-1} at 20.0 A g^{-1}	52.0%	[13]
---------------------------	---	-------	------

SUPPORTING INFORMATION

Table S3. The Warburg impedance coefficient (σ_w), the molar concentration of Na^+ (C) and diffusion coefficient of Na^+ (D_{Na}) of the $\text{SnS@C/MoS}_2@\text{N,P-C}$, SnS@C/MoS_2 and SnS@C electrodes.

Cycle numbers	Potential (V)	Electrodes	σ_w ($\Omega \text{ s}^{-1/2}$)	C (mol cm^{-3})	D_{Na} ($\text{cm}^2 \text{ s}^{-1}$)
50 Cycles	Charge to 2.6 V	$\text{SnS@C/MoS}_2@\text{N,P-C}$	188.9	1.94×10^{-3}	2.07×10^{-13}
		SnS@C/MoS_2	236.2	1.91×10^{-3}	1.37×10^{-13}
		SnS@C	415.3	2.39×10^{-3}	2.81×10^{-14}

References

- [S1] S. Zhang, G. Wang, Z. Zhang, B. Wang, J. Bai and H. Wang, 3D graphene networks encapsulated with ultrathin SnS nanosheets@hollow mesoporous carbon spheres nanocomposite with pseudocapacitance-enhanced lithium and sodium storage kinetics, *Small*, 2019, **15**, 1900565.
- [S2] H. Jia, M. Dirican, N. Sun, C. Chen, P. Zhu, C. Yan, X. Dong, Z. Du, J. Guo, Y. Karaduman, J. Wang, F. Tang, J. Tao and X. Zhang, SnS hollow nanofibers as anode materials for sodium-ion batteries with high capacity and ultra-long cycling stability, *Chem. Commun.*, 2019, **55**, 505-508.
- [S3] Y. Wang, Y. Zhang, J. Shi, A. Pan, F. Jiang, S. Liang and G. Cao, S-doped porous carbon confined SnS nanospheres with enhanced electrochemical performance for sodium-ion batteries, *J. Mater. Chem. A*, 2018, **6**, 18286-18292.
- [S4] J. Shi, Y. Wang, Q. Su, F. Cheng, X. Kong, J. Lin, T. Zhu, S. Liang and A. Pan, N-S co-doped C@SnS nanoflakes/graphene composite as advanced anode for sodium-ion batteries, *Chem. Eng. J.*, 2018, **353**, 606-614.
- [S5] J. Zhu, C. Shang, Z. Wang, J. Zhang, Y. Liu, S. Gu, L. Zhou, H. Cheng, Y. Gu and Z. Lu, SnS/SnSb@C nanofiber with enhanced cycling stability via vulcanization as anode for sodium ion batteries, *ChemElectroChem*, 2018, **5**, 1098-1104.
- [S6] X. Hu, J. Chen, G. Zeng, J. Jia, P. Cai, G. Chai and Z. Wen, Robust 3D macroporous structures with SnS nanoparticles decorating nitrogen-doped carbon nanosheet networks for high performance sodium-ion batteries, *J. Mater. Chem. A*, 2017, **5**, 23460-23470.
- [S7] Y. Zheng, T. Zhou, C. Zhang, J. Mao, H. Liu and Z. Guo, Boosted charge transfer in SnS/SnO₂ heterostructures: toward high rate capability for sodium-ion batteries, *Angew. Chem., Int. Ed.*, 2016, **55**, 3408-3413.
- [S8] L. Wu, H. Lu, L. Xiao, X. Ai, H. Yang and Y. Cao, Improved sodium-storage performance of stannous sulfide@reduced graphene oxide composite as high capacity anodes for sodium-ion batteries, *J. Power Sources*, 2015, **293**, 784-789.
- [S9] L. Wang, G. Yang, J. Wang, S. Peng, W. Yan and S. Ramakrishna, Controllable design of MoS₂ nanosheets grown on nitrogen-doped branched TiO₂/C nanofibers: toward enhanced sodium storage performance induced by pseudocapacitance behavior, *Small*, 2019, 1904589.
- [S10] M. Feng, M. Zhang, H. Zhang, X. Liu and H. Feng, Room-temperature carbon coating on MoS₂/Graphene hybrids with carbon dioxide for enhanced sodium storage, *Carbon*, 2019, **153**, 217-224.
- [S11] S. Chen, S. Huang, J. Hu, S. Fan, Y. Shang, M. E. Pam, X. Li, Y. Wang, T. Xu, Y. Shi and H. Y. Yang, Boosting sodium storage of Fe_{1-x}S/MoS₂ composite via heterointerface engineering, *Nano-Micro Lett.*, 2019, **11**, 80.
- [S12] P. Li, Y. Yang, S. Gong, F. Lv, W. Wang, Y. Li, M. Luo, Y. Xing, Q. Wang, and S. Guo, Co-doped 1T-MoS₂ nanosheets embedded in N, S-doped carbon nanobowls for high-rate and ultra-stable sodium-ion batteries, *Nano Res.*, 2019, **12**, 2218-2223.

SUPPORTING INFORMATION

[S13] Z. Li, S. Liu, B. P. Vinayan, Z. Zhao-Karger, T. Diemant, K. Wang, R. J. Behm, C. Kübel, R. Klingeler and M. Fichtner, Hetero-layered MoS₂/C composites enabling ultrafast and durable Na storage, *Energy Storage Mater.*, 2019, **21**, 115-123.